Torque-generating malaria-infected red blood cells in an optical trap

J.A. Dharmadhikari, S. Roy, A.K. Dharmadhikari, S. Sharma, and D. Mathur[#]

Tata Institute of Fundamental Research, 1 Homi Bhabha Road, Mumbai 400 005, India
[#]atmol1@tifr.res.in

Abstract: We have used optical tweezers to trap normal and *Plasmodium*-infected red blood cells (iRBCs). Two different facets of the behavior of RBCs in infrared light fields emerge from our experiments. Firstly, while the optical field modifies both types of RBCs in the same fashion, by folding the original biconcave disk into a rod-like shape, iRBCs rotate with linearly polarized light whereas normal RBCs do not. Secondly, and in the context of known molecular motors, our measurements indicate that the torque of rotating iRBCs is up to three orders of magnitude larger.

OCIS codes: (170.1420) Biology; (140.7010) Trapping; (170.4520) Optical confinement and manipulation.

References and Links

1. A. Ashkin, J.M. Dziedzic, J.E. Bjorkholm, and S. Chu, "Observation of a single-beam gradient force optical trap for dielectric particles," Opt. Lett. **11**, 288-290 (1986).
2. K. Schutze, G. Posl, and G. Lahr, "Laser micromanipulation systems as universal tools in cellular and molecular biology and in medicine," Cell. Mol. Biol. **44**, 735-746 (1998).
3. M. Zahn, and S. Seeger, "Optical tweezers in pharmacology," Cell. Mol. Biol. 44, 747-761 (1998).
4. A. Clement-Sengewald, K. Schutze, A. Ashkin, G.A. Palma, G. Kerlen, and G. Brem, "Fertilization of bovine oocytesinduced solely with combined laser microbeam and optical tweezers," J. Assisted Reproduction Genetics **13**, 259-265 (1996).
5. M. Zahn, J. Renken, and S. Seeger, "Fluorimetric multiparameter cell assay at the single cell level fabricated by optical tweezers," FEBS Lett. **443**, 337-340 (1999).
6. C. Bustamante, Z. Bryant, and S.B. Smith, "Ten years of tension: single-molecule DNA mechanics," Nature **421**, 423-427 (2003).
7. A. Krantz, "Red-cell mediated therapy: opportunities and challenges," Blood Cells, Molecules and Diseases **23**, 58-68 (1997).
8. J.P. Shelby, J. White, K. Ganeshan, P.K. Rathod, and D.T. Chiu, "A microfluidic model for single-cell capillary obstruction by *Plasmodium falcipuram*-infected erythrocytes," PNAS **100**, 14618-14622 (2003).
9. H.A. Cranston, C.W. Boylan, G.L. Carroll, S.P. Sutera, J.R. Williamson, I.Y. Gluzman, and D.J. Krogstad, "Plasmodium falcipuram maturation abolishes Physiologic Red cell deformability," Science **223**, 400-403 (1984).
10. H.G. Roggenkamp, F. Jung, R. Schneider, and H. Kiesewetter, "A new device for the routine measurement of erythrocyte deformability," Biorheology Suppl. **1**, 241-243 (1984).
11. R.A. Beth, "Mechanical detection and measurement of the angular momentum of light," Phys. Rev. **50**, 115-125 (1936).
12. M.E.J. Friese, J. Enger, H. Rubinsztein-Dunlop, and R.N. Heckenberg, "Optical angular-momentum transfer to trapped absorbing particles," Phys. Rev. A **54**, 1593-1596 (1996).
13. N.B. Simpson, K. Dholakia, N. Allen, and M.J. Padgett, "Mechanical equivalent of the spin and orbital angular momentum of light: an optical spanner," Opt. Lett. **22**, 52-54 (1997).
14. L. Paterson, M.P. MacDonald, J. Arlt, W. Sibbett, P.E. Bryant, and K. Dholakia, "Controlled rotation of optically-trapped microscopic particles," Science **292**, 912-914 (2001)
15. M.E.J. Friese, T.A. Nieminen, R.N. Heckenberg, and H. Rubinsztein-Dunlop, "Optical alignment and spinning of laser-trapped microscopic particles," Nature **394**, 348-350 (1998).
16. L.D. Landau, and E.M. Lifshitz, *Theory of elasticity*, (Pergamon Press, New York, 1959) p. 56.
17. S. Henon, G. Lenormand, A. Richert, and F. Gallet, "A new determination of the shear modulus of the human erythrocyte membrane using optical tweezers," Biophys. J. **76**, 1145-1151 (1999).
18. C. Duranton, S.M. Huber, V. Tanneur, K.S. Lang, B.B. Brand, C.D. Sandu, and F. Lang, "Electrophysiological properties of the *Plasmodium falciparum*-induced cation conductance of human erythrocytes," Cell Phys. Biochem. **13**, 189-198 (2003).
19. H.M. Staines, J.C. Ellory, and K. Kirk, "Perturbation of the pump-leak balance of Na^+ and K^+ in malaria-infected erythrocytes," Am. J. Physiol. Cell Physiol. **380**, C1575-C1587 (2001).

#3681 - $15.00 US Received 16 January 2004; revised 17 March 2004; accepted 17 March 2004

20. A.J. Hunt, F. Gittes, and J. Howard, "The force exerted by a single kinesin molecule against a viscous load," Biophys. J. **67**, 766-781 (1994).
21. C. Lambros, and J.P. Vanderberg, "Synchronization of *Plasmodium falciparum* erythrocytic stages in culture," J. Parasitol. **65**, 418-420 (1979).
22. F.F. Vargas, M.H. Osorio, U.S. Ryan, and M. De Jesus, "Surface charge of endothelial cells estimated from electrophoretic mobility," Membr. Biochem. **8**, 221-227 (1989).
23. B.T. Marshall, M. Long, J.W. Piper, T. Yago, R.P. McEver, and C. Zhu, "Direct observation of catch bonds involving cell-adhesion molecules," Nature 423, 190-193 (2003).
24. B.M. Cooke, N. Mohandas, and R.L. Coppel, "The malaria-infected red blood cell: structural and functional changes," Adv. Parasitol. **50**, 1-86 (2001).
25. K. Ley, "Integration of inflammatory signals by rolling neutrophils," Immunol. Rev. 186, 8-18 (2002).
26. H. Noji., R. Yasuda., M. Yoshida, and K. Kinosita, "Direct observation of the rotation of F_1-ATPase," Nature **386**, 299-302 (1997).
27. W.S. Ryu, R.M. Berry, and H.C. Berg, "Torque generating units of the flagellar motor of *Escherichia coli* have a high duty ratio," Nature **403**, 444-447 (2000).
28. K. Kinosita Jr., R.Yasuda, H. Noji, and K. Adachi, "A rotary molecular motor that can work at near 100% efficiency," Phil. Trans. Roy. Soc. London B **355**, 473-489 (2000).
29. A. Goswami, S. Singh, V.D. Redkar, and S. Sharma, "Characterization of P0, a ribosomal phosphoprotein of *Plasmodium falciparum*," J. Biol. Chem. **272**, 12138-12143 (1997).

1. Introduction

The ability of optical tweezers [1] to trap and manipulate single cells has opened new vistas for basic research in the life sciences, like single cell molecular biology [2], as well as for diverse applications ranging from laser-assisted in-vitro fertilization [3] and the development of cell biosensors [4] to new possibilities of micromanipulation of relevance to cell sorting and cellular microchips [4,5]. New insights have been forthcoming from application of optical tweezers to studies of the mechanics of single DNA molecules [6]. Optical trapping also makes feasible single-cell testing of erythrocytes that are linked to pharmacophores for use in drug therapy [7].

Over and above attempts to develop sensitive diagnostics for malaria, single-cell studies of normal and *Plasmodium*-infected red blood cells (RBCs) have assumed considerable importance in recent years [8] as it now appears established that malaria-induced organ failure is associated with capillary blockage and the enhanced rigidity of iRBCs. Elastometric microchannels of micron-sized diameters have been utilized to establish differences in deformability of normal and iRBCs [8]. Rheoscopes have also been used to visualize RBC deformability by relying on measurements of fluid shear stress [9]. Filtration experiments have been performed that relate the velocities of RBCs as they pass through micron-sized pores to cell area, volume and cytoplasmic viscosity [10].

In the context of cellular and molecular motors, following experiments conducted by Beth nearly 7 decades ago [11] that first demonstrated the development of torques in tiny quartz crystals in polarized light, much contemporary effort has been directed towards the use of optical tweezers to explore the possibility of driving micromachines by transferring angular momentum from light to micron-sized particles. The last few years has seen reports of light-induced motion of absorbing microscopic particles with elliptically polarized light [12], with laser beams possessing helical phase structure [13] or a Laguerre-Gaussian profile [14], and upon irradiation of birefringent micro-particles with circularly polarized light [15]. However, relatively little work on motors has been reported at a "real" cellular level.

We have made use of single-beam optical tweezers geometry to trap red blood cells with linearly polarized light. A strongly focused laser beam was used to generate gradient forces, F_g, that pull dielectric particles towards the focal zone whose magnitudes are larger than the scattering forces, F_s, that push the particles away from the focus, towards the incident light direction. The magnitude of the total force that is generated in our trap was $F = (F_s^2 + F_g^2)^{1/2}$. For laser power P, typically *ca.* 20 mW at the trap, the optical force, $F \sim P\, n/c$ (where n is the refractive index of the medium, and c is the speed of light), lies in the picoNewton range. We verified that this is sufficient to spatially trap an RBC against streaming velocities up to *ca.* 32 $\mu m\ s^{-1}$. The wavelength of the incident light in our trap, 1.064 μm, obtained from a TEM_{00}

#3681 - $15.00 US Received 16 January 2004; revised 17 March 2004; accepted 17 March 2004

mode diode-pumped Nd:YVO_4 laser, avoids optical damage to the trapped RBCs. We measured the light to be linearly polarized to better than one part in 10,000. A 100× large numerical aperture (NA=1.3) oil-immersed objective was used to create the trap. Direct imaging of the trapped cells enabled us to make real-time determinations of rotational speed and other trapping characteristics.

2. Results and discussion

Figure 1 shows how an infected RBC behaves in our optical trap. In panel a) the relative positions of an infected cell and the laser focus are marked. As the infected cell moves towards the laser focus, trapping occurs; this is accompanied by shape distortion such that, after a period of 2 s, the original disk-like RBC changes, by folding and twisting action, into a rod-like shape that rotates. We discuss the rotational motion in the following but note that in panels d) to f), the folded structure unfolds once the laser beam is removed. Unfolding times were found to be typically a factor of 4 larger than the characteristic folding time. Similar folding and unfolding behavior was also observed for uninfected RBCs. RBCs are normally fragile and rupture very easily. On regaining their original shape after removal of the trap, the RBCs did not rupture even after being kept at room temperature for several hours. Since red cells do not possess a nucleus and do not multiply, quantification of viability (or growth) is not possible in conventional terms.

The normal equilibrium shape of a human red blood cell (RBC) is a flattened biconcave disk whose diameter is about 7 μm, and whose thickness varies from about 0.9 μm at the thinnest central portion of the disk to 2.1 μm at the largest part near the periphery. The folding of the RBC that we observe is not inconsistent with its known morphology. The ratio

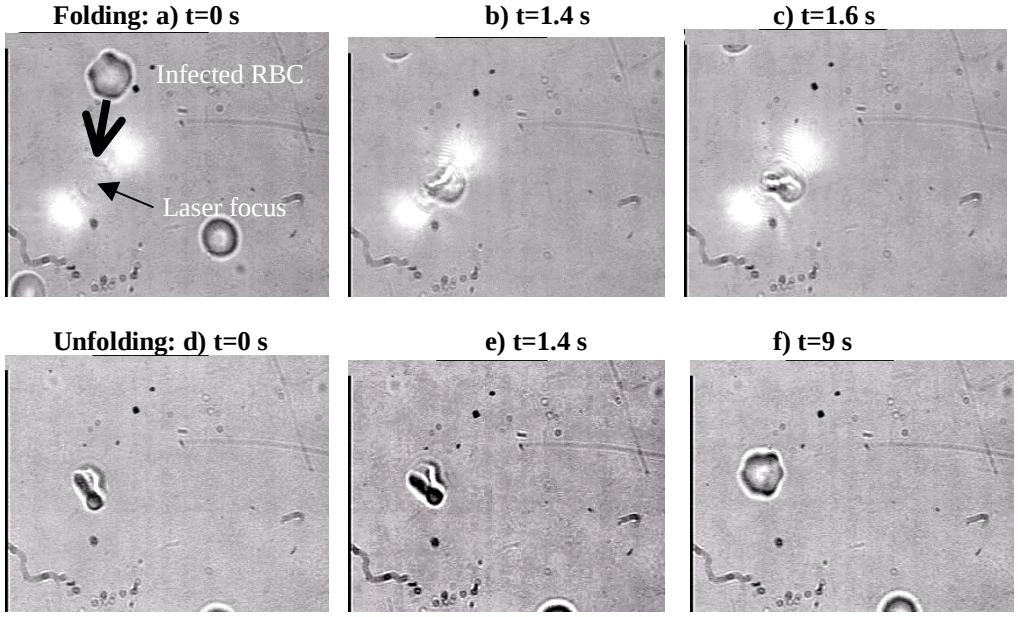

Fig. 1. Time evolution of folding (334 KB) and unfolding (1.04 MB) of red blood cells (RBCs) infected with *Plasmodium falciparum* [29] in an optical trap using a linearly polarized infrared laser. Panel a shows the initial state where an infected RBC approaches the laser focus (*ca.* 1 μm diameter). Panels b and c show the trapped RBC undergoing folding and twisting due to polarization-induced optical forces such that a rod-like shape is achieved within ~2 s. On removal of the laser beam, unfolding to the original shape occurs (panels d-f) on a longer time scale.

of volume to surface area for RBCs is smaller than in the case of a sphere. For identical surface areas, the ratio of the RBC volume to spherical volume is significantly less than unity

#3681 - $15.00 US Received 16 January 2004; revised 17 March 2004; accepted 17 March 2004

(*ca.* 0.6), so that energy constraints do not seriously impede RBCs from readily assuming different non-spherical shapes. The elastic response of an RBC to an applied force is likely to be determined essentially by the cell membrane as the inner fluid has no elasticity by virtue of it being purely viscous. In terms of two-dimensional laws of elasticity [16] the elastic shear modulus, μ, of the cell membrane and the area compressibility, K, determine the dynamics responsible for the observed morphological changes in the trapped RBCs. The elastic properties of the cytoskeleton determine the magnitude of μ while K is controlled by the almost incompressible phospholipidic bilayer. For RBCs, it is established [17] that $K>>\mu$. Thus, the folding and unfolding that is observed (Fig. 1) proceeds in such manner that the elastic properties of the cytoskeleton come into play while the overall area of the cytoskeleton remains constant.

We take an RBC to be a non-absorbing, asymmetric dielectric object. The linearly polarized light beam used to make our optical trap possesses an electric field, E, whose direction is well defined, and under easy control of the experimentalist. This field induces a dipole moment $\mathbf{p} = \boldsymbol{\alpha}.\mathbf{E}$, where $\boldsymbol{\alpha}$ is the polarizability tensor of the RBC whose intrinsic asymmetry implies that polarizability components parallel and perpendicular to the RBC axis ($\alpha_{//}$ and $\alpha_{\perp}$, respectively) are significantly different to each other. This difference comes into play in the resulting light-induced torque that is generated, $\boldsymbol{\tau} = \mathbf{p} \times \mathbf{E}$, such that energy minimization constraints induce in the trapped RBCs a "kick" in a direction that will lead to alignment along the direction of the **E**-field vector. Note that the anisotropy in polarizability for normal RBCs is not large enough to induce rotational motion with linearly polarized light. We have made measurements using a half-wave plate that enables us to alter the direction of the **E**-vector and we have confirmed that normal RBCs align themselves along this vector. Where does the enhanced anisotropy in $\boldsymbol{\alpha}$ originate in the case of iRBCs?

Recent electrophysiology experiments [18,19] have established that transport of Na^+, Ca^{2+} and K^+ ions is very significantly altered upon infection of RBC by *Plasmodium falciparum*; net Ca^{2+} entry into iRBCs is 18 times faster than in non-infected cells and is accompanied by exchange of K^+ by Na^+ in the cytosol. Although the functional significance of ion movement within iRBCs is not well understood at present, it is clear that the outwardly directed gradient of K^+ ions across the parasite plasma membrane will give rise to a K^+ diffusion potential within an iRBC [18]. Moreover, the Na^+ leak will also generate a Na^+ gradient across the cell parasite plasma membrane that will serve to drive Na^+-coupled transport, in the opposite direction, into the parasite cytosol. Differences in mobilities for the different ionic species are likely to increase the anisotropy of the polarizability tensor for iRBCs. Nevertheless, the gross morphology of the cell remains unaffected upon infection by *Plasmodium falciparum*. It is clear that cell shape is not important as both RBCs and iRBCs have the same shape but only the latter rotate in our experiments with linearly polarized light.

The dynamics of the rotational motion that such a "kick" initiates are expected to be governed by, among other factors, the hydrodynamic friction that is experienced by the rod-like trapped RBC. We characterize this in terms of a frictional drag coefficient, ξ that is given by [20]:

$$\xi = \frac{(\pi/3)\,\eta\,L^3}{\ln(L/2r) - 0.447},$$

where L is the length of the cylinder and r its width, and η is the viscosity of the medium (in N m^{-2} s). The rotational speed, ω (in rad. s^{-1}) is expressed in terms of ξ and the torque, Γ, by:

$$\Gamma = \omega\,\xi.$$

Figure 2 depicts selected time frames from a movie that shows typical rotational motion that is induced in an iRBC. Rotational speeds of iRBCs varied from 0.3 Hz (19 rpm) to 5 Hz (300 rpm), and appeared to depend on the stage of infection. *Plasmodium falciparum* infected red cells were synchronized [21] and the fastest rotation (5 Hz; 300 rpm) was observed for

#3681 - $15.00 US Received 16 January 2004; revised 17 March 2004; accepted 17 March 2004

cells 12-18 hours post-synchronization, which are at the early trophozoite stage. The slowest rotations were observed for the mature shizonts (40-48 hours post-synchronization) at a speed of 19 rpm. This is understandable since the infected red cells possess maximum anisotropy in the trophozoite stage. As the parasite matures to the segmented schizont stage, the infected cells become uniformly distributed with small cell bodies (merozoites), the red cell volume decreases and so does the anisotropy. The values of torque generated by the rotating iRBCs covered the range from 55,000 pN nm to 3300 pN nm. It is possible that the rotational speed depends upon a dynamic interplay between laser power and the infection stage. Further work is in progress to properly disentangle the two effects but present data indicate a linear dependence of rotational speed on laser power.

Might the rotation that we observe be due to some thermally mediated torque? We believe the answer to be in the negative. Angular momentum conservation would require that the surrounding medium circulate in a direction that is opposite to that of the rotating, trapped RBC. We have ample evidence that this is not the case. Indeed, our observations are that if a second RBC happens to encroach in the vicinity of a rotating trapped cell, it is also likely to be swept around in the same direction. This is consistent with our postulate of an externally (optically) driven trapped cell that also stirs the surrounding medium. Measurements lead us to believe that asymmetric light scattering is not significant in the rotation dynamics. This is a reasonable expectation as the scattering force will always act in the direction of light propagation whereas the rotations that we observe are in an orthogonal direction.

What might the generated torque imply for iRBCs? Obviously generation of torque on iRBCs through optical forces is unlikely *in vivo*. However, torques may arise *in vivo* due to i) the slightly charged surfaces of the endothelial cells [22], ii) fluid sheer forces of pN magnitude [23], and iii) the ionic anisotropy of iRBCs. Sequestration of infected erythrocytes in brain microvasculature contributes to cerebral malaria, a severe complication of *Plasmodium falciparum* infection [24]. The trophozoite and early schizont stages, which showed maximum torque in our experiments, are precisely the stages that exhibit adhesion to endothelial cells. For inflammation-mediated adhesion of leukocytes to the endothelial cells, braking movements (rolling) are known to be critical [25]. Leukocytes did not show any folding or rotation in our optical trap. Thus the mechanism of rolling of leukocytes is unlikely to be due to ionic anisotropy, and is probably caused by membrane tethering [23]. Since iRBC adhesion is a major determinant in cerebral malaria, further understanding of the anisotropies amongst normal and infected red cells is essential for understanding the differential behaviour of iRBCs inside capillaries.

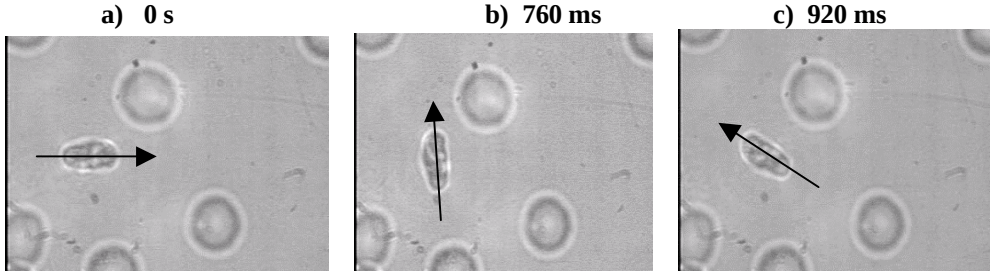

Fig. 2. Discrete frames from a movie (1.29 MB) depicting rotation of an infected RBC in the optical trap. The arrow helps identify the direction of rotation. Times associated with each frame are indicated; the speed of rotation was 120 revolutions per minute (rpm). The rotational speeds achieved in these experiments covered the range 19-300 rpm. The untrapped cells visible in the frames were outside the laser focus and underwent Brownian motion.

It is of interest to place the torque values that we have measured in the context of those for known molecular micromotors [26]. Molecular motors generate force between two cellular components. To date, two molecular motors are known that enable rotary motion to be accomplished: the bacterial flagellar motor that relies on proton flow as the energy source to

#3681 - $15.00 US Received 16 January 2004; revised 17 March 2004; accepted 17 March 2004

rotate a flagellum [27] and the F_0F_1-ATP synthase [28] that consists of two rotary motors, one that is driven by proton flow (known as the F_0 motor) and the other, the F_1 motor, whose energy is derived from ATP hydrolysis.

In the case of actin, it has been shown that for lengths of 1 μm, rotational speeds of 6 revs s^{-1} (*ca.* 40 rad. s^{-1}) are readily achieved [28], indicating the generation of torque that is of the order of 40 pN nm, a value that is very significantly smaller than that obtained with our iRBCs. Moreover, the motor that we invoke with iRBCs can be controlled to a larger extent

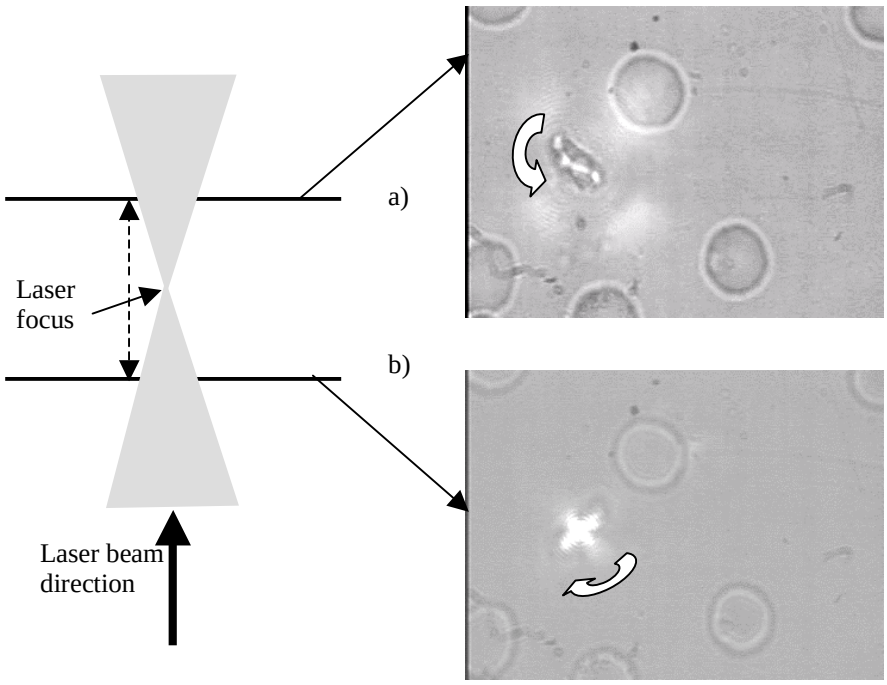

Fig. 3. Controlling the sense of rotation by altering the position of the infected RBC with respect to the focal plane of laser beam. If the cell is at position a), anti-clockwise rotation is observed (1.29 MB). The cell at position b) rotates in clockwise direction (1.20 MB). The rotational speeds remain the same as long as laser power does not change. The **k**-vector (see text) is along the laser propagation direction while the **E**-vector lies perpendicular to it but in the same plane.

than has hitherto been possible with flagellar and ATPase motors. Figure 3 shows that we are able to control the direction of rotation in our RBC-motor by positioning the RBC at different locations along the laser propagation direction. When the cells are at position a), slightly downstream of the focal plane, anti-clockwise rotations of the iRBCs are observed. On changing the position to b), slightly upstream of the focal plane, the rotation becomes clockwise, with the speed remaining the same. The measure of control is most likely a consequence of the change in direction with respect to the **E**-vector of that component of effective polarizability that lies out of the **k**-**E** plane although it is possible to also invoke alternative rationalization in terms of propeller-like action of rod-like iRBCs. We are not aware of similar control being possible in any other molecular or cellular micromotor, notwithstanding the fact that the motor mechanism in the former class of micromotors might well be somewhat different from those pertaining to the latter category.

#3681 - $15.00 US Received 16 January 2004; revised 17 March 2004; accepted 17 March 2004